GEOLOGY | THE GEOLOGICAL SOCIETY OF AMERICA®

https://doi.org/10.1130/G51223.1

Manuscript received 13 December 2022
Revised manuscript received 5 March 2023
Manuscript accepted 9 June 2023

Published online XX Month 2023

Discovery of Permian–Triassic eclogite in northern Tibet establishes coeval subduction erosion along an ~3000-km-long arc

Chen Wu[1,*], Andrew V. Zuza[2], Drew A. Levy[2,3], Jie Li[4], and Lin Ding[1]

[1]State Key Laboratory of Tibetan Plateau Earth System, Environment and Resources, Institute of Tibetan Plateau Research, Chinese Academy of Sciences, Beijing 100101, China

[2]Nevada Bureau of Mines and Geology, University of Nevada, Reno, Nevada 89557, USA

[3]Department of Geological Sciences, Jackson School of Geosciences, University of Texas at Austin, Texas 78712, USA

[4]Chongqing Key Laboratory of Complex Oil and Gas Filed Exploration and Development, Chongqing University of Science and Technology, Chongqing 401331, China

ABSTRACT

Eclogite bodies exposed across Tibet record a history of subduction-collision events that preceded growth of the Tibetan Plateau. Deciphering the time-space patterns of eclogite generation improves our knowledge of the preconditions for Cenozoic orogeny in Tibet and broader eclogite formation and/or exhumation processes. Here we report the discovery of Permo-Triassic eclogite in northern Tibet. U-Pb zircon dating and thermobarometry suggest eclogite-facies metamorphism at ca. 262–240 Ma at peak pressures of ~2.5 GPa. Inherited zircons and geochemistry show the eclogite was derived from an upper-plate continental protolith, which must have experienced subduction erosion to transport the protolith mafic bodies to eclogite-forming conditions. The Dabie eclogites to the east experienced a similar history, and we interpret that these two coeval eclogite exposures formed by subduction erosion of the upper plate and deep trench burial along the same ~3000-km-long north-dipping Permo-Triassic subduction complex. We interpret the synchroneity of eclogitization along the strike length of the subduction zone to have been driven by accelerated plate convergence due to ca. 260 Ma Emeishan plume impingement.

INTRODUCTION

Tectonic eclogite lenses generated by (ultra-) high-pressure [(U)HP] metamorphism commonly form during subduction-collision processes. Therefore, their occurrence provides unique insights into the tectonic evolution of an orogen and its physical-chemical conditions (Liou et al., 2004; Agard et al., 2009). Tectonic eclogites may develop from oceanic or continental mafic protoliths in a subduction and/or collisional setting. A subduction zone can generate Pacific-type eclogite via the subduction of oceanic crust (Yin et al., 2007; Agard et al., 2009) or the entrainment of continental material into a subduction trench due to subduction erosion (Nielsen and Marschall, 2017). Continental collisions can lead to deep subduction of the continental crust to generate Himalaya-type eclogite (Liou et al., 2004). The investigation of exposed eclogite lenses is crucial for reconstructing the kinematic evolution of ancient subduction-collisional orogens.

The Tibetan Plateau formed due to protracted oceanic subduction and continental collisions in the Phanerozoic. Sparse eclogite blocks observed across the plateau provide important records of the subduction-collision history (Yin et al., 2007). Tibet is comprised of continental strips that collided as part of the Tethyan orogen (Şengör, 1984). Northern Tibet exposes a series of east-trending suture zones and arc systems (Wu et al., 2016) that reflect the tectonic evolution of the Proto- and Paleo-Tethys orogens (Yang et al., 2009). Early Paleozoic eclogites widely distributed in northern Tibet are interpreted to be associated with the closure of the Proto-Tethys Ocean (Yang et al., 2009; Wei et al., 2009; Song et al., 2014; Liu et al., 2018) (Fig. 1). Despite the presence of a well-known Permo-Triassic arc in the Eastern Kunlun that accommodated north-dipping Paleo-Tethys oceanic subduction and later collision (Wu et al., 2016), no coeval (U)HP metamorphic rocks have been observed. Here, we make the first report of Permo-Triassic eclogite related to the Paleo-Tethys oceanic evolution. U-Pb zircon geochronology and geochemical analyses are presented to constrain the pressure-temperature-time (*P-T-t*) paths, formation age, protolith, and tectonic evolution of the eclogite. With our new observations, we argue for the development of a ~3000-km-long north-dipping Permo-Triassic subduction-collision zone that linked laterally with the Dabie orogen across central China.

GEOLOGICAL SETTING

Northern Tibet occupies a position between the Central Asian and the Tethyan orogenic systems, which experienced Neoproterozoic and Paleozoic orogeny and Cenozoic intraplate deformation (Yang et al., 2009; Wu et al., 2016; Zuza et al., 2018; Liu et al., 2018; Dong et al., 2021). The main tectonic units consist of the early Paleozoic Qilian orogen, Qaidam block, and Eastern Kunlun orogen (Fig. 1). Early Paleozoic arc plutons associated with the subduction-collision process of the Proto-Tethys Ocean were overprinted by a wide Permo-Triassic arc in the Kunlun-Qaidam region (Wu et al., 2016; Zuza et al., 2018; Dong et al., 2021). This north-dipping subduction zone consumed the Paleo-Tethys Ocean (Neo-Kunlun in some reconstructions) (Wu et al., 2016). The Kunlun suture records the final closure of this ocean and correlates eastward

Chen Wu https://orcid.org/0000-0003-0647-3530
*wuchen@itpcas.ac.cn

CITATION: Wu, C., et al., 2023, Discovery of Permian–Triassic eclogite in northern Tibet establishes coeval subduction erosion along an ~3000-km-long arc: Geology, v. XX, p. , https://doi.org/10.1130/G51223.1

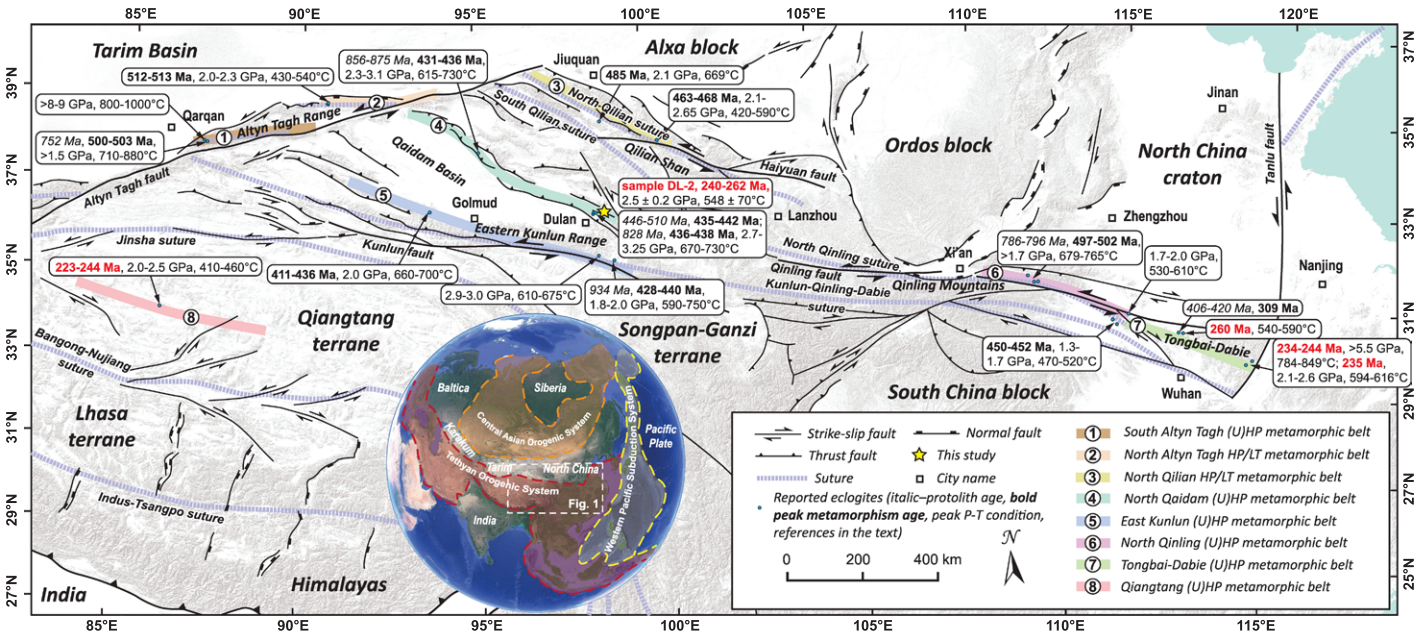

Figure 1. Map of northern Tibet and adjacent regions showing eclogite localities. The sample number and ages shown in red represent the Permian–Triassic eclogites. Data sources are Liu et al. (2018), Song et al. (2014), Yang et al. (2009), Liu et al. (2005), Pullen et al. (2008), and Cheng et al. (2013). Note the younger eclogites within the Bangong-Nujiang suture zone are not included. *P-T*—pressure-temperature; (U)HP—(ultra-)high-pressure; LT—low-temperature.

with the South Qinling suture (Hacker et al., 2004; Dong et al., 2021) (Fig. 1). Along strike to the east, the Dabie orogen was generated by the Late Triassic collision of the North China and South China blocks (Hacker et al., 2004; Liu et al., 2005).

Northern Tibet exposes a record of (U)HP eclogites that are mostly early Paleozoic in age, as found in the Altyn Tagh (Liu et al., 2018), North Qilian (Wei et al., 2009), North Qaidam (Song et al., 2014), Eastern Kunlun (Yang et al., 2009), and North Qinling (Dong et al., 2021) regions (Fig. 1). Reported Permo-Triassic (U)HP rocks are observed in the Dabie and Qiangtang belts of central Tibet (Liu et al., 2005; Pullen et al., 2008; Cheng et al., 2013) (Fig. 1).

METHODS AND RESULTS

We conducted a field investigation of eclogite bodies near Dulan city, northern Tibet, and collected samples of the eclogite and its host orthogneiss (location: 36.518°N, 98.614°E). The eclogite and related ultramafic blocks (i.e., pyroxene peridotite and dunite blocks) occur as boudin lenses ~40 m long and ~20 m wide, structurally mixed within strongly lineated (approximately N-trending) and deformed granitic gneiss (Fig. 2A). Two distinct eclogite samples were collected during two field trips, and mineral separation of these samples

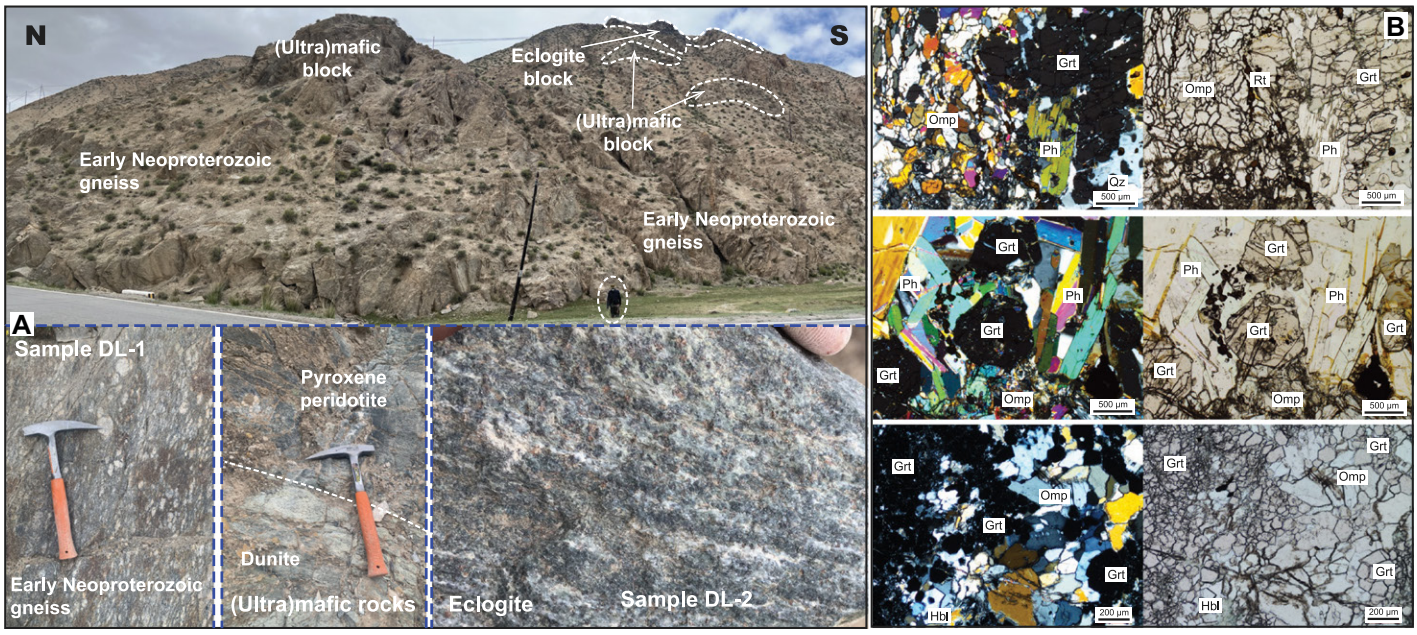

Figure 2. (A) Photographs of eclogite and ultramafic blocks within gneiss. (B) Left: photomicrographs in cross polarized light; right: plane polarized light: eclogite with mineral assemblages of garnet (Grt), omphacite (Omp), phengite (Ph), quartz (Qz), hornblende (Hbl), and rutile (Rt). Grt grains contain Omp inclusions; Omp grains are retrogressed.

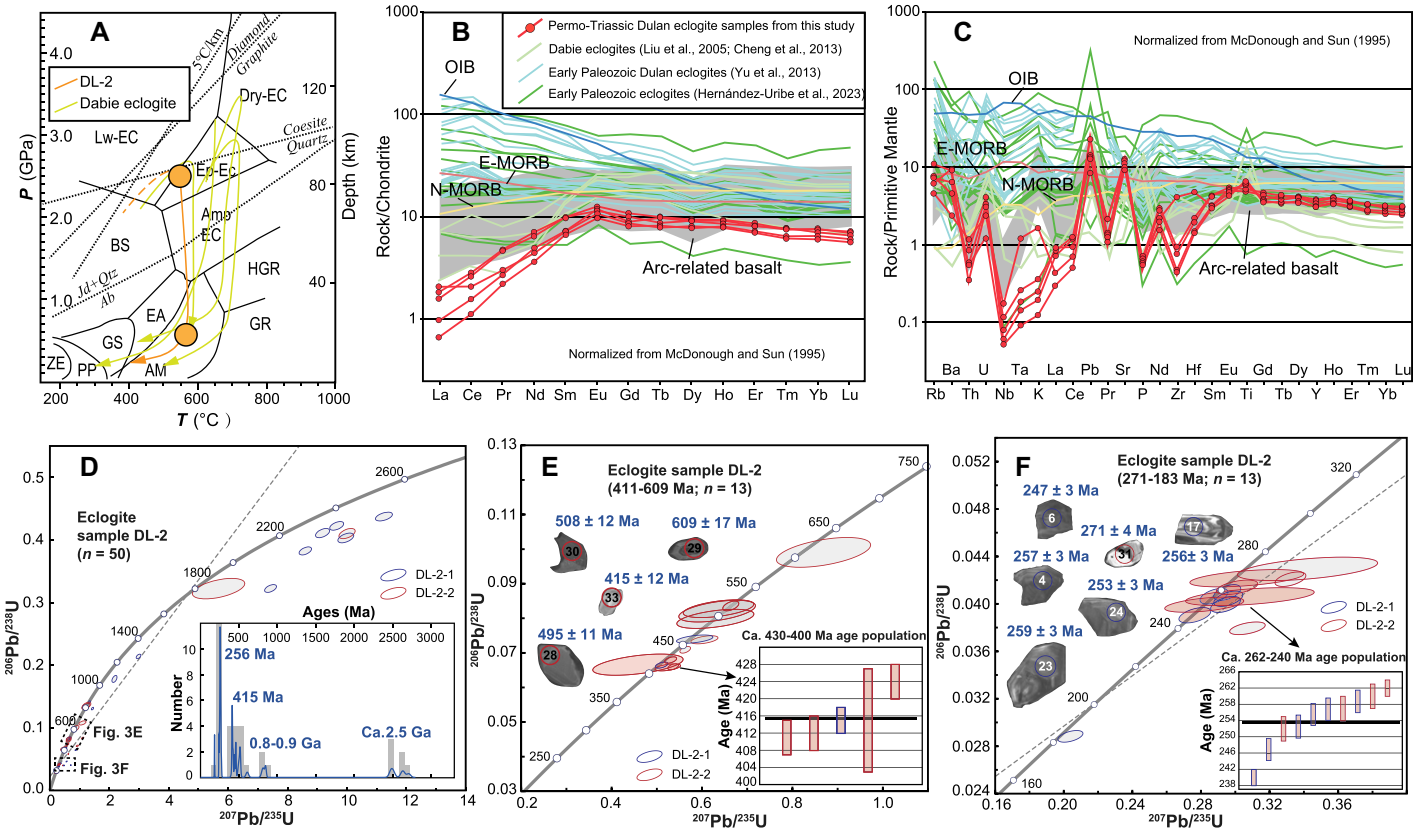

Figure 3. (A) Pressure-temperature (*P-T*) paths for Dulan and Dabie eclogite samples. Lw-EC—lawsonite eclogite facies; Dry-EC—dry eclogite facies; Ep-EC—epidote eclogite facies; BS—blueschist facies; Amp EC—amphibole eclogite facies; HGR—high-pressure granulite facies; GR—granulite facies; EA—epidote amphibolite facies; AM—amphibolite facies; GS—greenschist facies; PP—prehnite-pumpellyite facies; ZE—zeolite facies; Jd—jadeite; Qtz—quartz; Ab—albite. (B, C) Spider plots for the eclogite samples. OIB—ocean island basalt; N-MORB, E-MORB—normal and enriched mid-ocean-ridge basalt. (D–F) Zircon concordia plots of the Dulan eclogite; insets show representative cathodoluminescence images of analyzed zircons. Inset histograms: Fig. 3D, relative probability plot of zircon ages for eclogite sample; Figs. 3E and 3F: weighted mean calculation plots for different age populations. Circled numbers on the CL images are the sequence in zircon U-Pb dating in the laboratory corresponding to the numbers in supplementary age data.

occurred separately to assess and preclude sample contamination. The eclogite has heteroblastic textures with a mineral assemblage of garnet (~35 vol%), omphacite (~45%), phengite (~5%), quartz and rare plagioclase (~5%), and minor amphibole and rutile (Fig. 2B). Analytical methods and data for zircon dating, mineral analyses, whole-rock geochemistry, and Sr-Nd isotope analyses are in the Supplemental Material[1].

Garnets in the studied Dulan eclogite show homogenous compositions (Fig. S1 in the Supplemental Material). The X_{Mn} values decrease from core to rim, and X_{Mg} exhibits reversed zoning (Table S1). Omphacite shows uniform compositions (Fig. S1). Si contents in phengite vary from 6.74 to 6.89 atoms per formula unit (Table S1). Matrix amphibolite is retrogressed, with a relatively wide range of compositional variations, which is mostly magnesio-hornblende (Fig. S1). Two stages of metamorphism were identified. The peak-stage metamorphism had a mineral assemblage of garnet + omphacite + rutile + phengite. Garnet-omphacite-phengite thermobarometry (Krogh Ravna and Terry, 2004) suggests near-UHP conditions of $P = 2.5 \pm 0.2$ GPa and $T = 548 \pm 70$ °C (Fig. 3A). Coesite was not observed. A subsequent retrograde metamorphism occurred at amphibolite facies conditions with addition of H_2O. Amphibolite facies retrogression occurred at $P = \sim 0.6$ GPa and $T = 567 \pm 18$ °C determined by amphibole thermobarometry (Gerya et al., 1997). The eclogite records a clockwise decompression path (Fig. 3A).

The eclogite samples are characterized by (1) low SiO_2, K_2O, and Na_2O; (2) high MgO, Fe_2O_3, CaO, Al_2O_3, and TiO_2 (Table S2); (3) slight light rare earth element (REE) depletion; (4) flat heavy REE pattern with a slight positive Eu anomaly (Fig. 3B); (5) low initial $^{87}Sr/^{86}Sr$ (0.704338–0.704688); and (6) high εNd (6.13–8.16) (Table S3). Samples are enriched in large ion lithophile elements (Rb, Ba, Sr) and depleted in high field strength elements (Nb, Ta, P) (Fig. 3C), with low $(La/Yb)_N$ values (0.10–0.34), Zr contents, and Zr/Y ratios (<3.3) (Table S2). This geochemistry overlaps fields for subduction-related arc basalts (Xia, 2014) but is dissimilar from that of the other reported early Paleozoic eclogite bodies near Dulan (Yu et al., 2013; Hernández-Uribe et al., 2023) (Figs. 3B and 3C).

The mylonitic gneiss sample DL-1 yielded a 944 ± 11 Ma U-Pb zircon date interpreted as the protolith crystallization age, with some younger Neoproterozoic–early Paleozoic metamorphic Pb loss (Fig. S2). Zircon dating of eclogite sample DL-2 included 26 grains from subsample DL-2-1 and 24 grains from subsample DL-2-2, which yielded diverse, mostly concordant ages that span 2646 Ma to 183 Ma with four distinct age populations (Fig. 3D). The similarity of ages of two subsamples of sample DL-2 confirms data reproducibility (Table S4). We interpret that the two older ca. 2.5 Ga and 0.9 Ga discordant-age populations represent inherited zircons from a Neoarchean basement intruded by ca. 0.9 Ga plutons or related Pb loss. A significant population of zircons spans 430–400 Ma (Fig. 3E), which overlaps the ages of early Paleozoic arc plutons observed in the Qaidam

[1]Supplemental Material. Methods, Figures S1–S4, and Tables S1–S4. Please visit https://doi.org/10.1130/GEOL.S.23519067 to access the supplemental material, and contact editing@geosociety.org with any questions.

terrane (Wu et al., 2016). The early Paleozoic dates have Th/U values >0.1, consistent with a magmatic origin (Fig. S3), and we interpret these dates to best reflect the eclogite protolith age. The youngest age population ($n = 12$) spans 262 ± 2 Ma to 240 ± 2 Ma (Fig. 3F) with Th/U ratios <0.1 that decrease with younger ages (Fig. S3). Zircon dates may reflect peak eclogite conditions or late-stage exhumation (Hernández-Uribe et al., 2023). We interpret that the spread of ages reflects protracted metamorphism ca. 262–240 Ma.

DISCUSSION

The Permo-Triassic Dulan eclogite has a significant component of inherited zircons that suggests the protolith rocks intruded and assimilated continental crust to incorporate older zircon. The xenocrystic ca. 2.5 Ga and 0.9 Ga zircon age populations are consistent the local bedrock geology of the Qaidam terrane (Yu et al., 2013), including our dating of the host gneiss. The ca. 430–400 Ma zircons are coeval with the Proto-Tethys arc that formed along the southern margin of Qaidam (Wu et al., 2016). We interpret that arc-related basalt generated during ca. 430–400 Ma north-dipping subduction intruded the Qaidam basement to generate the eclogite protolith (Fig. 4A), which is supported by the geochemical data (Figs. 3B and 3C). Subsequent opening of the Paleo-Tethys Ocean occurred during rifting of the Songpan-Ganzi terrane (Şengör, 1984; Wu et al., 2016) (Fig. 4B).

The ca. 262–240 Ma metamorphic zircon dates bracket the timing of protracted eclogitization, which coincides with activity of the north-dipping Permo-Triassic Paleo-Tethys arc that developed along Qaidam's southern margin (Fig. 4C). We interpret that mafic intrusions were transported from the continental margin by Permo-Triassic subduction erosion to >80 km depths to generate eclogite. The mechanism that exhumed the eclogite to the mid-crust is not well constrained. In the field, we observed strongly sheared Devonian terrestrial rocks around Dulan, including top-to-the-north normal-sense deformation and Devonian strata faulted atop gneiss. This deformation suggests detachment faulting occurred after the Devonian, but the complex structural relationships, including Cenozoic thrust and strike-slip faulting (e.g., Zuza et al., 2018), require further investigation. However, we interpret that the eclogite bodies were accreted to the base of the Qaidam terrane via diapirism and/or relamination (Yin et al., 2007; Hacker et al., 2011), resulting in penetrative stretching of the eclogite and host gneiss, and that these rocks were further exhumed to mid-crustal levels during slab rollback and upper-plate extension. Slab rollback is supported by southward-younging Triassic arc granites, ca. 225–195 Ma extension-related plutons, and thinning crustal thickness trends (Wu et al., 2016) (Fig. 4D).

The ca. 262–240 Ma Dulan eclogite is located ~100 km north of the Permo-Triassic Kunlun arc and suture zone, which requires that the subducted (U)HP rocks were emplaced to the mid-crust far within the plate interior. These observations are similar to those of the Qiangtang HP metamorphic belt in central Tibet and the North American Cordillera where subducted upper-plate rocks were underthrust hundreds of kilometers more inboard into the continental interior, with final exhumation caused by detachment faulting (Pullen et al., 2008; Pullen and Kapp, 2014; Chapman et al., 2020). The studied Permo-Triassic eclogites were found in close proximity to early Paleozoic eclogite with very different geochemical characteristics and zircon ages (Yu et al., 2013; Hernández-Uribe et al., 2023) (Figs. 3B and 3C). This observation suggests that these eclogite bodies with distinct tectonic histories were formed and exhumed by different events to a similar mid-crust position, where they sat for protracted periods of time

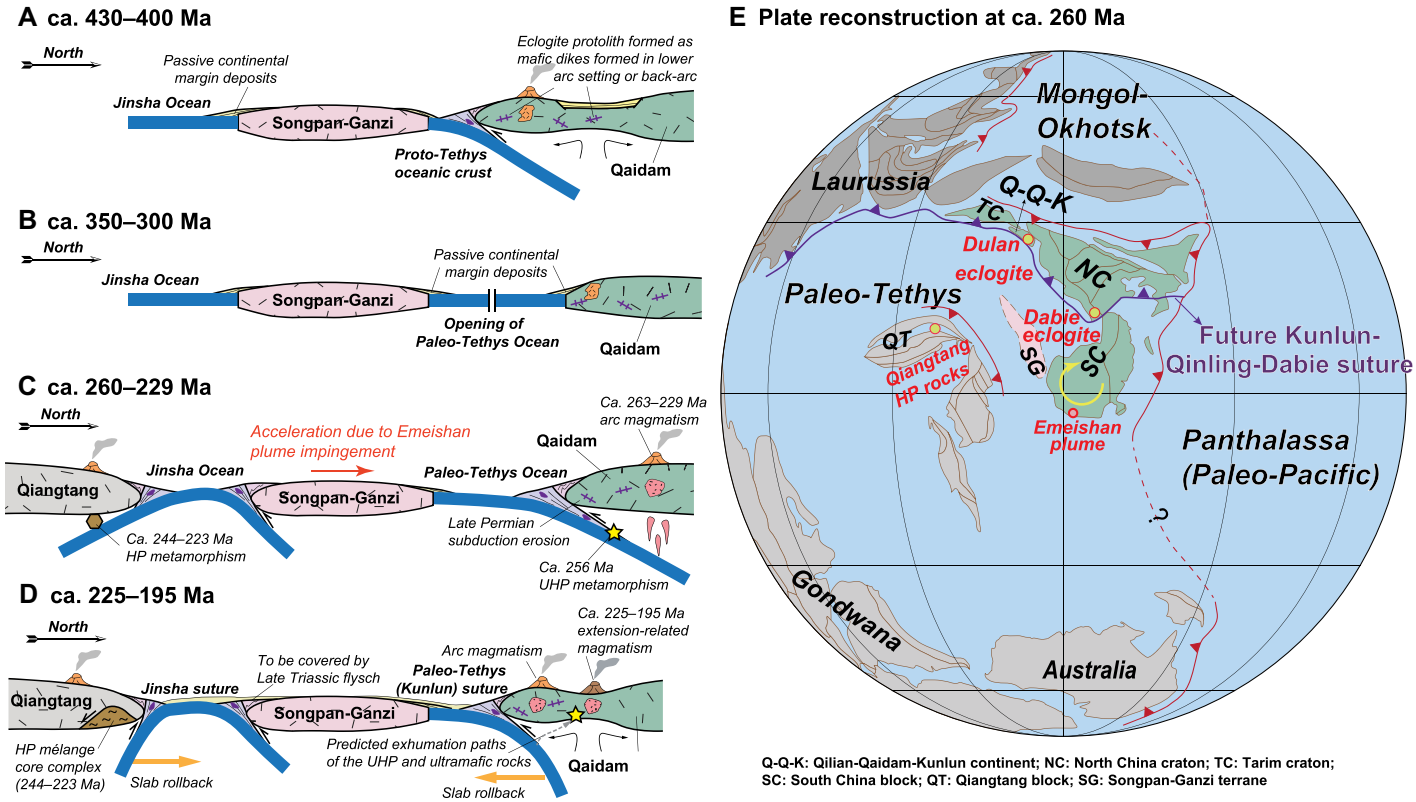

Figure 4. (A–D) Tectonic models for early Paleozoic protolith of eclogite formed within the Proto-Tethys arc before later collision (A), Carboniferous opening of the Paleo-Tethys Ocean (B), formation of (ultra-)high-pressure [(U)HP] metamorphic rocks during subduction of the oceanic lithosphere (C), and exhumation of the (U)HP rocks from deep to mid-crustal depths during slab rollback of the oceanic lithosphere (D). (E) Plate reconstruction at ca. 260 Ma (modified from Huang et al., 2018). The circular yellow arrow represents the rotation direction of the South China block during the closure of the Paleo-Tethys ocean.

(Menold et al., 2016) before their final exhumation during Mesozoic–Cenozoic deformation (Yin et al., 2007). The spatial overlap between the Permo-Triassic and early Paleozoic (U)HP rocks confirms that the Tibetan Plateau consists of relict suture zones that experienced repeated phases of overprinting orogenesis, consistent with a Wilson cycle evolution of the Tethyan orogenic system (Wu et al., 2016). In both the North American Cordillera and Tibet, the spatial position of HP rocks clearly does not uniquely reflect the configuration of ancient suture zones but rather the final configuration of overprinting processes.

The ca. 262–240 Ma Dulan eclogite shares similar characteristics with the Permo-Triassic Dabie eclogites to the east (Liu et al., 2005; Cheng et al., 2013) (Figs. 3A–3C). The Dabie orogen was generated by northward oceanic subduction beneath the North China continent and subsequent continental collision with South China evidenced by UHP metamorphism and Mesozoic post-collisional magmatism (Hacker et al., 2004). The protolith to Dabie UHP eclogites originated from the upper plate (i.e., the North China craton) as evidenced by inherited zircon populations and geochemistry (Zheng et al., 2006), and the rocks experienced eclogite-facies conditions from ca. 260 to 235 Ma before exhumation to the mid-crust (Hacker et al., 2004; Liu et al., 2005; Cheng et al., 2013). Based on the similarities between the Dabie and Dulan eclogites, including synchronous ages, protoliths derived from the upper-plate mafic intrusions, and burial via north-dipping subduction, we interpret that these eclogites formed along a linked ~3000-km-long north-dipping Permo-Triassic subduction zone established across central China (Fig. 4E). The geologic histories of the Kunlun, Qinling, and Dabie regions are similar along strike (Fig. S4).

Both the Dulan and Dabie eclogites require subduction erosion to have transported upper-plate material to (U)HP depths within the subduction trench at very similar times. Based on observed age constraints, this was not a continuous process during the life of the subduction system. Instead, we suggest that a punctuated event caused enhanced subduction erosion and the transportation of crustal materials to eclogite-faces depths synchronously along the Kunlun-Dabie arc system. A synthesis of data from modern subduction zones shows that fast plate-convergence rates enhance subduction erosion (Stern, 2011), and therefore, the punctuated synchronous formation of the Dabie and Dulan eclogites may have resulted from faster convergence rates and subduction erosion in the Permo-Triassic. One mechanism that may have increased plate-convergence rates is plume-induced push by the ca. 260 Ma Emeishan plume that impinged on South China (Liu et al., 2021) (Fig. 4E). Studies of the Mesozoic–Cenozoic India-Africa-Asia plate configuration demonstrate how mantle plumes can lead to accelerated plate-convergence rates and rotation (Cande and Stegman, 2011; van Hinsbergen et al., 2011, 2021). Although speculative, impingement of the Emeishan plume may have accelerated the northward motion of the South China plate and connected Paleo-Tethys lithosphere, driving its clockwise rotation relative to North China (Zhao and Coe, 1987). This model explains the increased convergence rates to drive subduction erosion and eclogitization of upper-plate rocks along the ~3000-km-long subduction system and the initiation of significant Middle–Late Triassic rotation of the South China block relative to North China during its diachronous collision with westward-propagating suturing (ca. 242–220 Ma; Liu et al., 2015). We envision that the South China–North China collision changed inter-plate dynamics to initiate southward rollback along the western Kunlun arc segment and northward rollback along the Qiangtang subduction belt (Pullen et al., 2008), ultimately exhuming HP rocks from diverse subduction systems to the middle crust.

ACKNOWLEDGMENTS

This research was supported by the Second Tibetan Plateau Science Expedition and Research Program (2019QZKK0708), Basic Science Center for Tibetan Plateau Earth System (41988101), and the National Science Foundation (EAR1914501). We thank editor Rob Strachan, and T. Kusky, P. Kapp, and an anonymous reviewer for constructive reviews.

REFERENCES CITED

Agard, P., Yamato, P., Jolivet, L., and Burov, E., 2009, Exhumation of oceanic blueschists and eclogites in subduction zones: Timing and mechanisms: Earth-Science Reviews, v. 92, p. 53–79, https://doi.org/10.1016/j.earscirev.2008.11.002.

Cande, S.C., and Stegman, D.R., 2011, Indian and African plate motions driven by the push force of the Reunion plume head: Nature, v. 475, p. 47–52, https://doi.org/10.1038/nature10174.

Chapman, A.D., Rautela, O., Shields, J., Ducea, M.N., and Saleeby, J., 2020, Fate of the lower lithosphere during shallow-angle subduction: The Laramide example: GSA Today, v. 30, no. 1, p. 4–10, https://doi.org/10.1130/GSATG412A.1.

Cheng, H., Zhang, C., Vervoort, J.D., and Zhou, Z.Y., 2013, New Lu–Hf and Sm–Nd geochronology constrains the subduction of oceanic crust during the Carboniferous–Permian in the Dabie orogen: Journal of Asian Earth Sciences, v. 63, p. 139–150, https://doi.org/10.1016/j.jseaes.2012.04.012.

Dong, Y.P., Sun, S.S., Santosh, M., Zhao, J., Sun, J.P., He, D.F., Shi, X.H., Hui, B., Cheng, C., and Zhang, G.W., 2021, Central China orogenic belt and amalgamation of East Asian continents: Gondwana Research, v. 100, p. 131–194, https://doi.org/10.1016/j.gr.2021.03.006.

Gerya, T.V., Perchuk, L.L., Triboulet, C., Audren, C., and Sez'ko, A.I., 1997, Petrology of the Tumanshet Zonal Metamorphic Complex, Eastern Sayan: Petrology, v. 5–6, p. 503–533.

Hacker, B.R., Ratschbacher, L., and Liou, J.G., 2004, Subduction, collision and exhumation in the ultrahigh-pressure Qinling-Dabie orogen, *in* Malpas, J., et al., eds., Aspects of the Tectonic Evolution of China: Geological Society, London, Special Publication 226, p. 157–175, https://doi.org/10.1144/GSL.SP.2004.226.01.09.

Hacker, B.R., Kelemen, P.B., and Behn, M.D., 2011, Differentiation of the continental crust by relamination: Earth and Planetary Science Letters, v. 307, p. 501–516, https://doi.org/10.1016/j.epsl.2011.05.024.

Hernández-Uribe, D., Mattinson, C.G., Regel, M.E., Zhang, J.X., Stubbs, K.A., and Kylander-Clark, A.R.C., 2023, Protracted eclogite-facies metamorphism of the Dulan area, North Qaidam ultrahigh-pressure terrane: Insights on zircon growth during continental subduction and collision: Journal of Metamorphic Geology, v. 41, p. 557–581, https://doi.org/10.1111/jmg.12708.

Huang, B.C., Yan, Y.G., Piper, J.D.A., Zhang, D.H., Yi, Z.Y., Yu, S., and Zhou, T.H., 2018, Paleomagnetic constraints on the paleogeography of the East Asian blocks during Late Paleozoic and Early Mesozoic times: Earth-Science Reviews, v. 186, p. 8–36, https://doi.org/10.1016/j.earscirev.2018.02.004.

Krogh Ravna, E.J., and Terry, M.P., 2004, Geothermobarometry of UHP and HP eclogites and schists—An evaluation of equilibria among garnet–clinopyroxene–kyanite–phengite–coesite/quartz: Journal of Metamorphic Geology, v. 22, p. 579–592, https://doi.org/10.1111/j.1525-1314.2004.00534.x.

Liou, J.G., Tsujimori, T., Zhang, R.Y., Katayama, I., and Maruyama, S., 2004, Global UHP metamorphism and continental subduction/collision: The Himalayan model: International Geology Review, v. 46, p. 1–27, https://doi.org/10.2747/0020-6814.46.1.1.

Liu, L., Zhang, J.F., Cao, Y.T., Green, H.W., II, Yang, W.Q., Xu, H.J., Liao, X.Y., and Kang, L., 2018, Evidence of former stishovite in UHP eclogite from the South Altyn Tagh, western China: Earth and Planetary Science Letters, v. 484, p. 353–362, https://doi.org/10.1016/j.epsl.2017.12.023.

Liu, S.F., Qian, T., Li, W.P., Dou, G.X., and Wu, P., 2015, Oblique closure of the northeastern Paleo-Tethys in central China: Tectonics, v. 34, p. 413–434, https://doi.org/10.1002/2014TC003784.

Liu, Y.C., Li, S.G., Xu, S.T., Jahn, B.M., Zheng, Y.F., Zhang, Z.G., Jiang, L.L., Chen, G.B., and Wu, W.P., 2005, Geochemistry and geochronology of eclogites from the northern Dabie Mountains, central China: Journal of Asian Earth Sciences, v. 25, p. 431–443, https://doi.org/10.1016/j.jseaes.2004.04.006.

Liu, Y.D., Li, L., van Wijk, J., Li, A.B., and Fu, Y.Y.V., 2021, Surface-wave tomography of the Emeishan large igneous province (China): Magma storage system, hidden hotspot track, and its impact on the Capitanian mass extinction: Geology, v. 49, p. 1032–1037, https://doi.org/10.1130/G49055.1.

Menold, C.A., Grove, M., Sievers, N.E., Manning, C.E., Yin, A., Young, E.D., and Ziegler, K., 2016, Argon, oxygen, and boron isotopic evidence documenting $^{40}Ar_E$ accumulation in phengite during water-rich high-pressure subduction metasomatism of continental crust: Earth and Planetary Science Letters, v. 446, p. 56–67, https://doi.org/10.1016/j.epsl.2016.04.010.

McDonough, W.F., and Sun, S.-s., 1995, The composition of the Earth: Chemical Geology, v. 120, p. 223–253, https://doi.org/10.1016/0009-2541(94)00140-4.

Nielsen, S.G., and Marschall, H.R., 2017, Geochemical evidence for mélange melting in global arcs: Science Advances, v. 3, https://doi.org/10.1126/sciadv.1602402.

Pullen, A., and Kapp, P., 2014, Mesozoic tectonic history and lithospheric structure of the Qiangtang terrane: Insights from the Qiangtang metamorphic belt, central Tibet, *in* Nie, J., et al., eds., Toward an Improved Understanding of Uplift Mechanisms and the Elevation History of the Tibetan Plateau: Geological Society of America Special Paper 507, p. 71–87, https://doi.org/10.1130/2014.2507(04).

Pullen, A., Kapp, P., Gehrels, G.E., Vervoort, J.D., and Ding, L., 2008, Triassic continental subduction in central Tibet and Mediterranean-style closure of the Paleo-Tethys Ocean: Geology, v. 36, p. 351–354, https://doi.org/10.1130/G24435A.1.

Şengör, A.M.C., 1984, The Cimmeride Orogenic System and the Tectonics of Eurasia: Geological Society of America Special Paper 195, 82 p., https://doi.org/10.1130/SPE195.

Song, S.G., Niu, Y.L., Su, L., Zhang, C., and Zhang, L.F., 2014, Continental orogenesis from ocean subduction, continent collision/subduction, to orogen collapse, and orogen recycling: The example of the North Qaidam UHPM belt, NW China: Earth-Science Reviews, v. 129, p. 59–84, https://doi.org/10.1016/j.earscirev.2013.11.010.

Stern, C.R., 2011, Subduction erosion: Rates, mechanisms, and its role in arc magmatism and the evolution of the continental crust and mantle: Gondwana Research, v. 20, p. 284–308, https://doi.org/10.1016/j.gr.2011.03.006.

van Hinsbergen, D.J.J., Steinberger, B., Doubrovine, P.V., and Gassmöller, R., 2011, Acceleration and deceleration of India-Asia convergence since the Cretaceous: Roles of mantle plumes and continental collision: Journal of Geophysical Research, v. 116, B06101, https://doi.org/10.1029/2010JB008051.

van Hinsbergen, D.J.J., et al., 2021, A record of plume-induced plate rotation triggering subduction initiation: Nature Geoscience, v. 14, p. 626–630, https://doi.org/10.1038/s41561-021-00780-7.

Wei, C.J., Yang, Y., Su, X.L., Song, S.G., and Zhang, L.F., 2009, Metamorphic evolution of low-*T* eclogite from the North Qilian orogen, NW China: Evidence from petrology and calculated phase equilibria in the system NCKFMASHO: Journal of Metamorphic Geology, v. 27, p. 55–70, https://doi.org/10.1111/j.1525-1314.2008.00803.x.

Wu, C., Yin, A., Zuza, A.V., Zhang, J.Y., Liu, W.C., and Ding, L., 2016, Pre-Cenozoic geologic history of the central and northern Tibetan Plateau and the role of Wilson cycles in constructing the Tethyan orogenic system: Lithosphere, v. 8, p. 254–292, https://doi.org/10.1130/L494.1.

Xia, L.Q., 2014, The geochemical criteria to distinguish continental basalts from arc related ones: Earth-Science Reviews, v. 139, p. 195–212, https://doi.org/10.1016/j.earscirev.2014.09.006.

Yang, J.S., Xu, Z.Q., Zhang, J.X., Zhang, Z.M., Liu, F.L., and Wu, C.L., 2009, Tectonic setting of main high- and ultrahigh-pressure metamorphic belts in China and adjacent region and discussion on their subduction and exhumation mechanism: Acta Petrologica Sinica, v. 25, p. 1529–1560.

Yin, A., Manning, C.E., Lovera, O., Menold, C.A., Chen, X.H., and Gehrels, G.E., 2007, Early Paleozoic tectonic and thermomechanical evolution of ultrahigh-pressure (UHP) metamorphic rocks in the northern Tibetan Plateau, northwest China: International Geology Review, v. 49, p. 681–716, https://doi.org/10.2747/0020-6814.49.8.681.

Yu, S.Y., Zhang, J.X., Li, H.K., Hou, K.J., Mattinson, C.G., and Gong, J.H., 2013, Geochemistry, zircon U-Pb geochronology and Lu-Hf isotopic composition of eclogites and their host gneisses in the Dulan area, North Qaidam UHP terrane: New evidence for deep continental subduction: Gondwana Research, v. 23, p. 901–919, https://doi.org/10.1016/j.gr.2012.07.018.

Zhao, X.X., and Coe, R.S., 1987, Palaeomagnetic constraints on the collision and rotation of North and South China: Nature, v. 327, p. 141–144, https://doi.org/10.1038/327141a0.

Zheng, Y.F., Zhao, Z.F., Wu, Y.B., Zhang, S.B., Liu, X.M., and Wu, F.Y., 2006, Zircon U–Pb age, Hf and O isotope constraints on protolith origin of ultrahigh-pressure eclogite and gneiss in the Dabie orogen: Chemical Geology, v. 231, p. 135–158, https://doi.org/10.1016/j.chemgeo.2006.01.005.

Zuza, A.V., Wu, C., Reith, R.C., Yin, A., Li, J.H., Zhang, J.Y., Zhang, Y.X., Wu, L., and Liu, W.C., 2018, Tectonic evolution of the Qilian Shan: An early Paleozoic orogen reactivated in the Cenozoic: Geological Society of America Bulletin, v. 130, p. 881–925, https://doi.org/10.1130/B31721.1.

Printed in the USA